Time Difference of Arrival on Contrast-Enhanced Ultrasound in Distinguishing Benign Inflammation From Malignant Peripheral Pulmonary Lesions

Min Tang[1†], Qianrong Xie[2†], Jiasi Wang[2†], Xiaoyu Zhai[3†], Hong Lin[4], Xiaoxue Zheng[1], Guoli Wei[1], Yan Tang[1], Fanwei Zeng[1], Yanpeng Chu[2], Jianqiong Song[1*], Jianqiang Cai[5*] and Fanxin Zeng[2*]

[1] Department of Ultrasound Imaging, Dazhou Central Hospital, Dazhou, China, [2] Department of Clinical Research Center, Dazhou Central Hospital, Dazhou, China, [3] Key Laboratory of Carcinogenesis and Translational Research (Ministry of Education/Beijing), Department of Thoracic Medical Oncology, Peking University Cancer Hospital and Institute, Beijing, China, [4] Department of Public Health Information, Sichuan Center for Disease Control and Prevention, Chengdu, China, [5] Department of Hepatobiliary Surgery, National Cancer Center/Cancer Hospital, Chinese Academy of Medical Sciences and Peking Union Medical College, Beijing, China

Introduction: Worldwide, the incidence and mortality of lung cancer are at the highest levels, and the most lesions are located in the lung periphery. Despite extensive screening and diagnosis, the pathologic types of peripheral pulmonary lesions (PPLs) are difficult to diagnose by noninvasive examination. This study aimed to identify a novel index—time difference of arrival (TDOA)—to discriminate between benign inflammation and malignant PPLs.

Methods: Using contrast-enhanced ultrasound (CEUS), we retrospectively analyzed 96 patients with PPLs who had undergone biopsy to confirm the pathologic types. All data were collected from Dazhou Central Hospital between December 2012 and July 2019. The parameters of CEUS were analyzed by two assistant chief physicians of ultrasound diagnosis. Area under the receiver operating characteristic curve analysis, sensitivity, specificity, positive predictive value, and negative predictive value were calculated to assess the diagnostic ability of different indices.

Results: We found that the TDOA significantly distinguished benign inflammation from malignant lesions. The TDOA was markedly increased in patients with malignant lesions than benign inflammation lesions ($P < 0.001$). Compared with conventional time-intensity curve (TIC) indices, TDOA showed high diagnostic accuracy (area under the curve = 0.894). Moreover, conventional diagnostic indices did not affect the diagnostic performance of TDOA by adjusting the receiver operating characteristic curve.

Conclusion: TDOA is feasible for the diagnosis of benign inflammation and malignant PPLs.

Keywords: contrast-enhanced ultrasound, peripheral pulmonary lesions, time difference of arrival, benign inflammation lesions, malignant lesions

INTRODUCTION

Lung cancer is one of the most common malignant tumors in the world with the highest incidence and mortality (1). According to the location of the tumor, lung cancer is divided into central type and peripheral type. Peripheral lung cancer accounts for about 70% of all lung cancer types and is difficult to be diagnosed with no obvious symptoms (2). The 5-year survival rate of lung cancer is about 70%–90% in the early stage (3–5), but approximately 75% patients are first diagnosed only in an advanced stage (6).

Common clinical methods such as dynamic contrast-enhanced magnetic resonance imaging (7), contrast-enhanced computed tomography (8, 9), low-dose computed tomography (10), and bronchoscopy (11) are used to diagnose the lung lesions. However, these methods have obvious diagnostic shortcomings, such as exposure to heavy dose of radiation (12), high cost (13, 14), and high false positive rates (15, 16). Some studies also have shown that the diagnostic capability of bronchoscopy is significantly reduced because of the increase in distance from the hilum and the small volume of tumor (17–19). Therefore, it is essential to improve the current screening and diagnostic ability.

Peripheral pulmonary lesions (PPLs) are close to the pleura, which can be easily detected by ultrasound. Contrast-enhanced ultrasound (CEUS) is a novel technique for real-time observation of disease states by using microbubble-based contrast agents (20, 21). CEUS has found application in many conditions such as myocardial inflammation (22), type I diabetes (23), carotid plaque (24), chronic kidney disease (25), and metastatic liver disease (9). A previous study has showed that the wash-in slope, time to peak intensity (TTP) and mean transit time (MTT) analyzed by CEUS can be used to distinguish the difference between malignant thoracic injuries and benign lesions (26). However, the low sensitivity and specificity of these conventional parameters for diagnosing PPLs by time intensity curves (TICs) analysis limits the application of CEUS.

In this study, we aimed to identify a novel index to diagnose the PPLs. For this purpose, we systematically analyzed the clinical data of 96 patients with PPLs and evaluated the efficacy of using time difference of arrival (TDOA) to distinguish between benign inflammation and malignant lesions.

MATERIALS AND METHODS

Patients

We retrospectively analyzed 324 patients with PPLs who had undergone CEUS and biopsy or histopathologic examination in our hospital between December 2012 and July 2019. The inclusion criteria were as follows: i) Age from 18 to 85 years old; ii) With contrast ultrasound and biopsy or histopathologic examination; iii) Under contrast conditions, all patients with peripulmonary lesions significantly enhanced after contrast-enhanced ultrasound compared with those without contrast medium injection were hypervascular lesions. The exclusion criteria were as follows: i) Patients with bleeding tendency, severe cardiac insufficiency, pulmonary hypertension, aortic aneurysm, mental disorders, and other causes of pulmonary insufficiency; ii) Patients allergic to contrast media, with poor physical condition and not cooperating with researchers. All patients were diagnosed by biopsy. 96 patients of them were
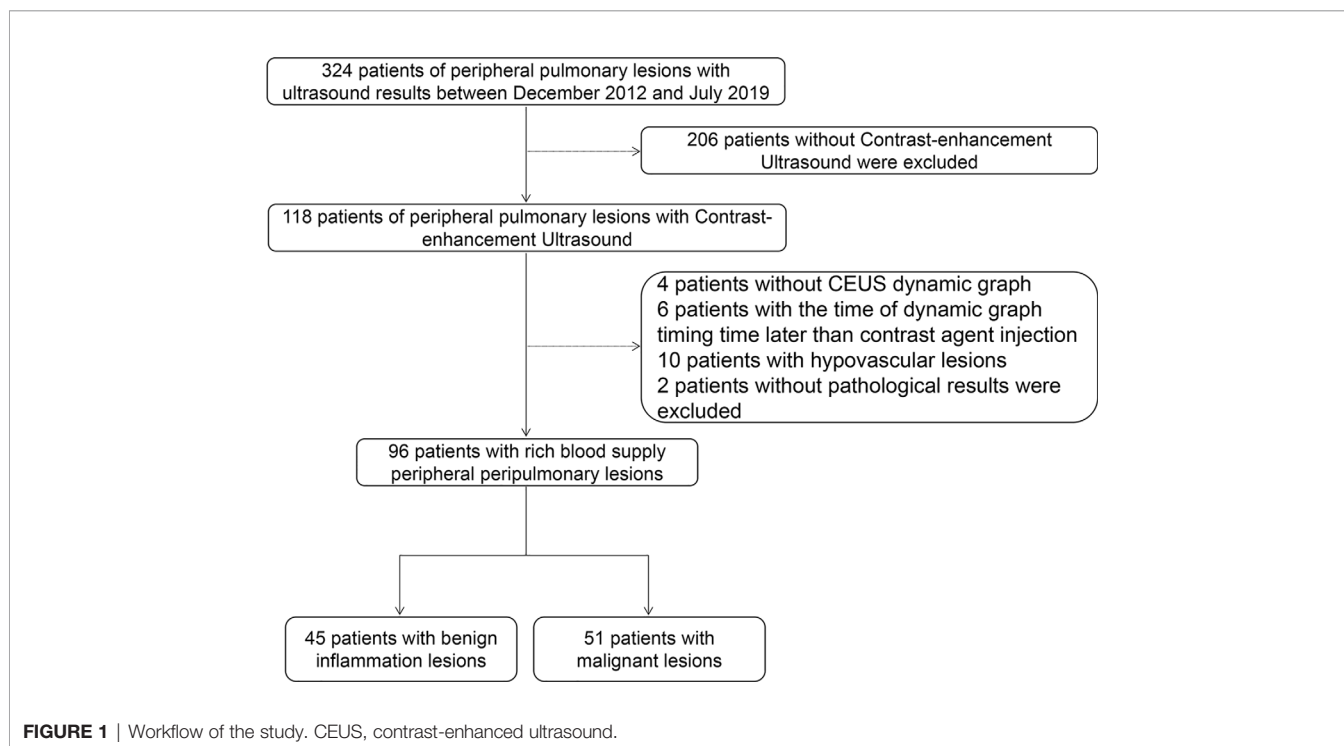

FIGURE 1 | Workflow of the study. CEUS, contrast-enhanced ultrasound.

TABLE 1 | Characteristics of 96 patients with peripheral pulmonary lesions.

	Benign inflammation lesions (N = 45)	Malignant lesions (N = 51)
Male gender, n (%)	32 (71.1)	39 (76.5)
Age, year, mean (SE)	59.5 (2.18)	63.9 (1.01)
Left lung, n (%)	22 (48.9)	31 (60.8)
Smoking, n (%)		
Current/Former	26 (57.8)	33 (64.7)
Never	18 (40.0)	17 (33.3)
Unclearly	1 (2.22)	1 (1.96)
Alcohol consumption, n (%)		
Never	21 (46.7)	25 (49.0)
Frequently/Occasionally	22 (48.9)	25 (49.0)
Unclearly	2 (4.4)	1 (1.96)
Medical history, n (%)		
Hypertension	7 (15.6)	7 (13.7)
Diabetes	4 (8.89)	4 (7.84)
Pulmonary diseases	4 (8.89)	4 (7.84)
Malignant tumors	1 (2.22)	3 (5.88)
Pathologic types, n (%)		
Nonspecific inflammation	37 (82.2)	—
Specific inflammation	8 (17.8)	—
Squamous cell carcinoma	—	23 (45.1)
Adenocarcinoma	—	21 (41.2)
Other	0	7 (13.7)

SE, standard error. There was no significant difference among the groups (P > 0.05).

included in this study and their ages ranged from 20 to 85 years (**Figure 1**, **Table 1**). Of the 96 patients, 45 had benign inflammation lesions: 37 (82.2%) and eight (17.8%) cases of nonspecific and specific inflammation, respectively. The remaining 51 patients had malignant lesions: 23 (45.1%) cases of squamous cell carcinoma and 21 (41.2%) of adenocarcinoma; the remaining seven (13.7%) patients had other malignancies. Patients were predominantly male (71.1% in the benign inflammation lesions group and 76.5% in the malignant lesions group). Left lung lesions accounted for 48.9% and 60.8% lesions in the benign inflammation and malignant lesions groups, respectively. There were no significant differences in demographic characteristics between the benign inflammation and malignant lesions groups (**Table 1**). The study was approved by the ethics committee of Dazhou Central Hospital (IRB00000003-19008).

Analysis of CEUS Parameters

A LOGIQ-E9 color Doppler ultrasonic diagnostic apparatus equipped with CEUS software, TIC analysis software, and a 3.5–5 MHz probe (GE Healthcare, Milwaukee, WI) were used in this study. The contrast agent for injection was white powder sulfur hexafluoride microbubble (SonoVue) for injection (Bracco SpA, Milan, Italy). Five milliliters physiological saline (0.9% NaCl) was added and agitated to form a microbubble suspension. We used conventional ultrasound to observe the size of the lesion, internal echo, and blood flow. Then, we placed the largest section of the lesion in the center of the display to initiate a double-contrast CEUS mode. Briefly,

2.4 mL sulfur hexafluoride microbubble suspensions were rapidly injected *via* the elbow vein, followed by a rapid bolus injection of 5 mL normal saline. The built-in timer of the ultrasound instrument was activated and observed for 3 min. All images were stored and analyzed.

Two assistant chief physicians with 5 years' experience in ultrasound diagnosis who were blinded to the pathological diagnosis of the patient, observed the filling characteristics of the contrast agent in the lesion and performed the CEUS analysis together and reached an agreement. First, we observed the blood supply in the mass and the area where the large vessels were located, distinguished the active area from the necrotic area, traced the real part of the lesion and the adjacent lung tissue as the regions of interest (ROI), and ensured the same ROI in each depiction. Then, the TIC software that comes with the LOGIQ-E9 color Doppler ultrasound was used to quantitatively analyze the arrival time (AT) of the lesion and adjacent lung tissues. Next, we obtained the values TDOA (in triplicate) of time difference between the AT of the lesion and adjacent lung tissue (=lesion contrast agent AT-adjacent lung tissue contrast agent AT), TTP, initial intensity (II), peak intensity (PI), area under the curve (AUC), rake ratio (K), mean square error (MSE), and curve gradient and calculated the average. After the analysis, the receiver operating characteristic (ROC) curve of adjacent lung tissue, lesion contrast agent AT and TDOA were drawn. The Youden's index was calculated to determine the best cut-off point of lesion AT and adjacent lung tissue time difference. If the arrival time was greater than the best cut-off point, the lesion was considered malignant; otherwise, it was considered benign inflammation.

Puncture Biopsy

A physician with > 5 years' experience performed the ultrasound biopsy of all patients. Infection markers, bleeding, and coagulation time of patients were required to be normal. The blood supply and large vessels in the mass were observed, and the puncture point was located in the area with blood supply but not large vessels. During the operation, the puncture point was fixed, the distance from the sampling point in the mass was measured, the puncture area was disinfected with iodine tincture, and the puncture point was anesthetized with 2% lidocaine for local infiltration. Next, under the guidance of contrast-enhanced ultrasound, an 18G automatic biopsy gun was used for subcutaneous penetration. The obtained specimens were fixed in 10% formaldehyde solution and sent for pathological examination.

Statistical Analysis

Quantitative data were expressed as mean (standard error [SE]), and the difference between groups was analyzed by student's *t*-test. The categorical data were expressed as numerical percentages. When theoretical frequency $1 \leq N < 5$, continuous correction chi-square test was used, and Pearson chi-square test was used for all theoretical frequencies n > 5. The sensitivity and specificity of the optimal cut-off point were calculated from the area under the

ROC curve. The ROC curve constructed from logistic regression and the ROC-AUC difference was analyzed by the DeLong's test. $P < 0.05$ was considered statistically significant. All the statistical methods were two tailed. The free degree of t-test for age, long diameter, and arrival time was 94, while the free degree of t-test for other parameters produced by the TIC analysis was 80.

RESULTS

Ultrasound Characteristics

The mean long diameter was 5.54 cm for the benign inflammation lesions group and 7.71 cm for the malignant lesions group ($P < 0.001$). Benign inflammation lesions were mainly wedge shaped, while malignant lesions were mainly spherical ($P < 0.001$). However, the conventional two-dimensional ultrasound indicators were not specific enough for the differential diagnosis of benign inflammation and malignant lesions. In this study, the PI, II, TTP, AUC, K, MSE, and gradient values could only be obtained from 34 and 48 patients with benign inflammation and malignant lesions, respectively. Furthermore, we found that the perfusion method, TTP, and PI produced by CEUS also showed no difference between the benign inflammation and malignant lesions groups ($P > 0.05$) (**Table 2**).

TABLE 2 | CEUS parameters of 96 patients with peripheral pulmonary lesions.

	Benign inflammation lesions (N = 45)	Malignant lesions (N = 51)	*P*-value
Two-dimensional ultrasound			
Long diameter (cm), mean (SE)	5.54 (0.26)	7.71 (0.40)	< 0.001
Lesion shape, n (%)			< 0.001
Wedge	26 (57.8)	4 (7.84)	
Irregular	14 (31.1)	20 (39.2)	
Spherical	5 (11.1)	27 (52.9)	
Bronchial tree sign, n (%)	7 (15.6)	6 (11.8)	0.59
CEUS			
Perfusion method, n (%)			0.22
Even perfusion	26 (57.8)	23 (45.1)	
Perfusion defect	19 (42.2)	28 (54.9)	
TIC analysis, mean (SE)			
Lesion AT (s)	5.54 (0.44)	8.69 (0.51)	< 0.001
Adjacent lung tissue AT (s)	4.45 (0.38)	4.65 (0.38)	0.71
Time difference of arrival (s)	1.09 (0.20)	4.03 (0.29)	< 0.001
Peak intensity (dB)[a]	23.8 (1.29)	22.3 (1.03)	0.34
Initial intensity (dB)[a]	-66.9 (4.30)	-66.8 (2.99)	0.99
Time to peak (s)[a]	17.5 (2.14)	14.5 (1.49)	0.24
Area under the curve[a]	1895 (88.9)	1802 (74.6)	0.42
Rake ratio[a]	4.50 (0.47)	4.59 (0.42)	0.88
Mean-square error[a]	9.41 (1.22)	7.81 (0.75)	0.24
Gradient[a]	1.89 (0.19)	2.05 (0.16)	0.52

[a]*Only 34 benign inflammation lesion patients and 48 malignant lesion patients had the peak intensity, initial intensity, time to peak, area under the curve, rake ratio, mean-square error and gradient value.*

CEUS, contrast-enhanced ultrasound; TIC, time-intensity curve; AT, arrival time.

Diagnostic Performance Comparison of Arrival Time

Based on TIC analysis, we generated the lesion AT, adjacent lung tissue AT, and a novel method of TDOA. The lesion AT and TDOA in the benign inflammation lesions group was shorter than those of the malignant lesions group ($P < 0.001$), but there was no difference in the adjacent lung tissue AT between both groups (**Figure 2** and **Figure S1**). TDOA had the largest area under the curve (AUC, 0.894), compared with the lesion arrival time (AUC, 0.785) and adjacent lung tissue arrival time (AUC, 0.495) (**Figure 3**). The optimal cut-off value of TDOA was 2.42 s. The sensitivity and specificity of TDOA were 86.3% (95% CI: 76.5–94.1) and 88.9% (95% CI: 80.0–97.8), respectively. Positive predictive value (PPV) and negative predictive value (NPV) were 85.1% (95% CI: 71.7–93.8) and 89.8% (95% CI: 77.8–96.6), respectively (**Table 3**). The PPV and NPV of TDOA were higher than the lesion AT and adjacent lung tissue AT.
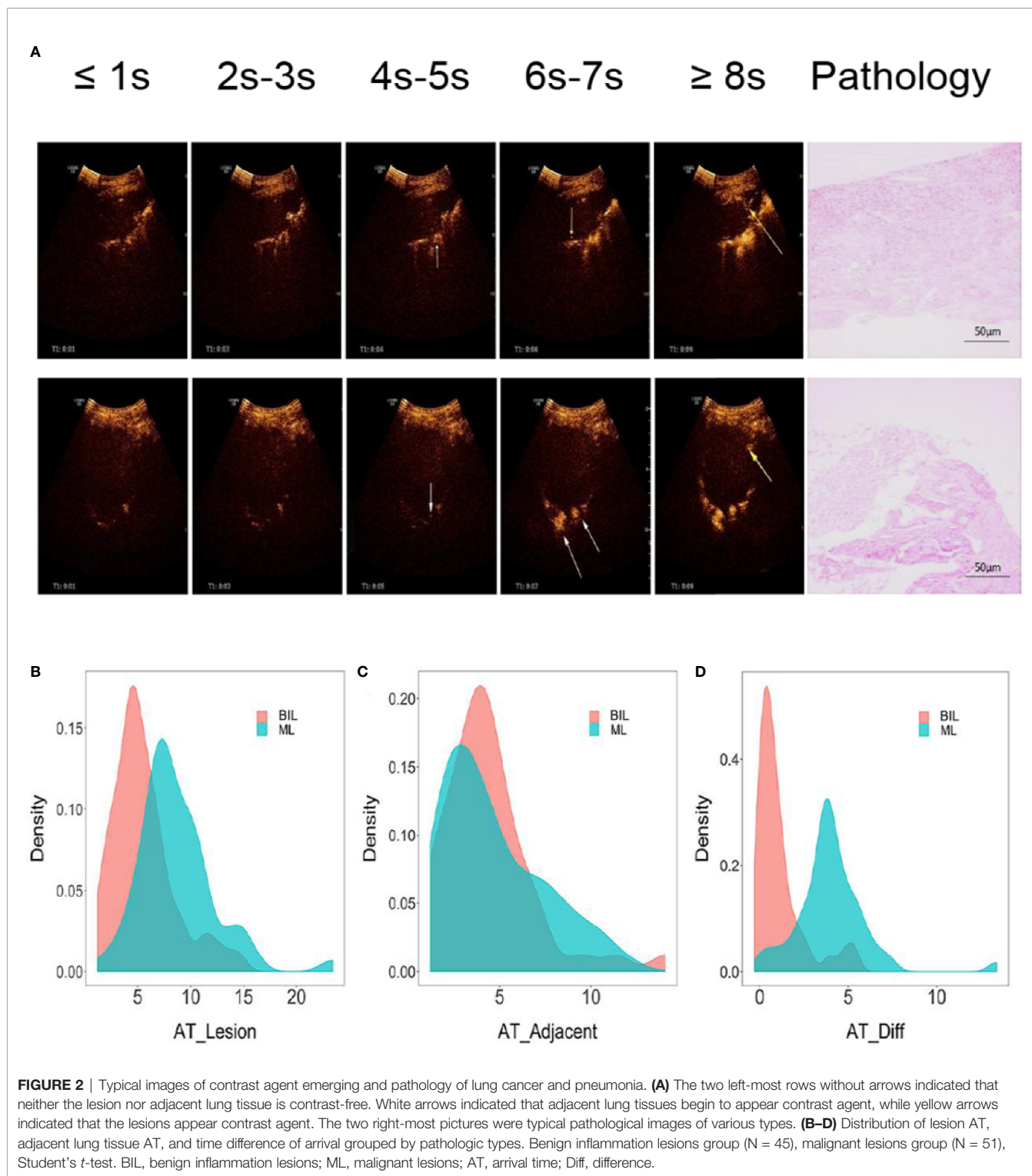
ROC Curve of TDOA Adjusted by the Index of Patients

To evaluate whether other CEUS parameters or clinical information affected the prediction performance of TDOA, we used different indicators to adjust the ROC curve. The adjusted ROC curve showed that other indicators such as age or TTP did not affect the diagnostic performance of TDOA (**Figure 4** and **Figure S2**). Next, we investigated the role of AT in the subgroup analysis. The results showed that the lesion AT and adjacent lung tissue AT could not distinguish between non-specific and specific inflammation. Significantly, TDOA could differentiate between the two groups well (**Figure S3**). However, all AT parameters did not distinguish between squamous cell carcinoma and adenocarcinoma (**Figure S4**).

DISCUSSION

Although many imaging technologies have been used to diagnose the PPLs, there are considerable limitations, especially in terms of diagnostic capability (17), cost (13), and radiation exposure (12), which pose challenges to PPLs diagnosis. In this study, we identified a novel method for the differential diagnosis of benign inflammation and malignant PPLs using TDOA produced by CEUS. Our results showed that the TDOA was significantly increased in the malignant lesions group than the benign inflammation lesions group. Notably, conventional diagnostic parameters did not affect the diagnostic performance of TDOA.

Previous study has indicated that CEUS divides the arterial phases into pulmonary and bronchial in the PPLs, and the pulmonary artery phase is slightly earlier than the bronchial artery phase (27). In this study, we found that the TDOA of the malignant lesions group (4.03 s) was significantly longer than the benign inflammation lesions group (1.09 s). This finding is

FIGURE 2 | Typical images of contrast agent emerging and pathology of lung cancer and pneumonia. **(A)** The two left-most rows without arrows indicated that neither the lesion nor adjacent lung tissue is contrast-free. White arrows indicated that adjacent lung tissues begin to appear contrast agent, while yellow arrows indicated that the lesions appear contrast agent. The two right-most pictures were typical pathological images of various types. **(B–D)** Distribution of lesion AT, adjacent lung tissue AT, and time difference of arrival grouped by pathologic types. Benign inflammation lesions group (N = 45), malignant lesions group (N = 51), Student's *t*-test. BIL, benign inflammation lesions; ML, malignant lesions; AT, arrival time; Diff, difference.

supported by previous studies that showed that the blood supply of malignant tumors mainly originates from the bronchial artery, while the blood supply of non-neoplastic pulmonary lesions comes from the pulmonary and bronchial arteries (28).

A large body of evidence has debated the value of CEUS in diagnosing lung diseases (29, 30). We found that TDOA produced by CEUS could well distinguish between benign inflammation and malignant lesions (AUC: 0.894). In addition,
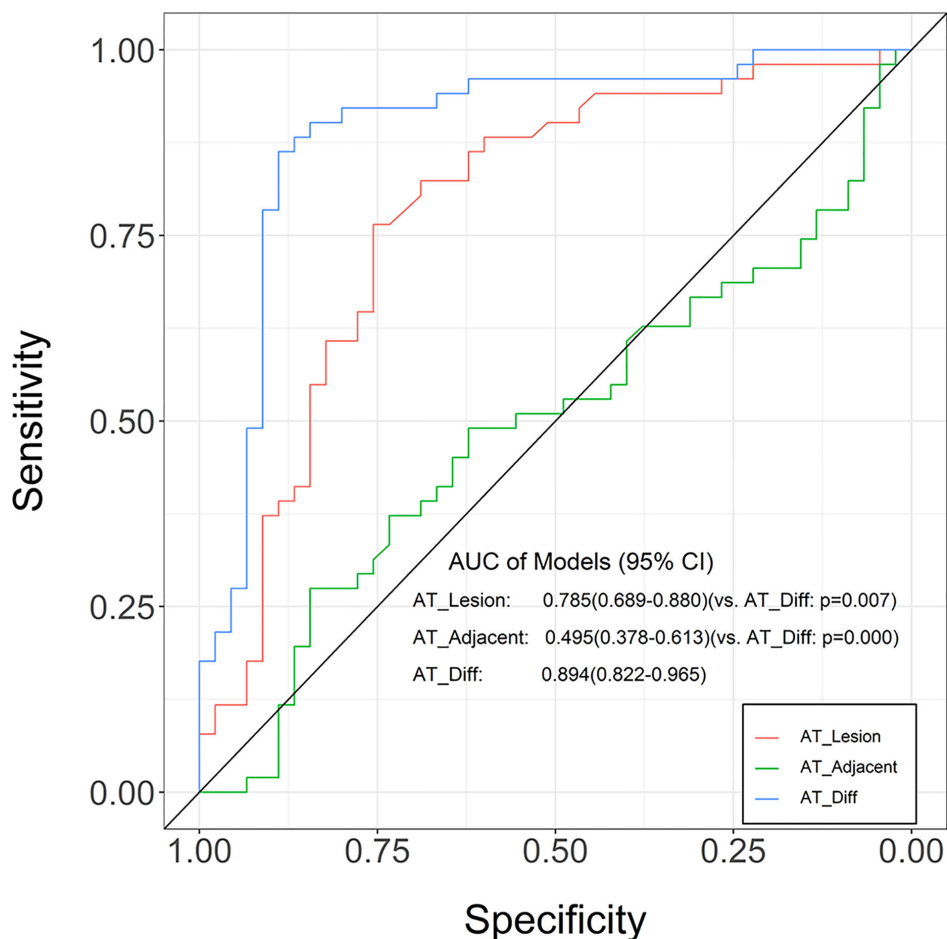
FIGURE 3 | Receiver operating characteristic (ROC) curves for the lung tissue AT, lesion AT, and time difference of arrival in distinguishing between benign inflammation and malignant lesions. Compared with adjacent lung tissue AT and lesion AT, the time difference of arrival was greater in AUC. The ROC curve is expressed by diagnostic sensitivity and specificity. AT, arrival time; Diff, difference.

TABLE 3 | Diagnostic performance of lesion AT, adjacent lung tissue AT, and time difference of arrival in benign inflammation lesions and malignant lesions group.

Items	AT_Lesion	AT_Adjacent	AT_Diff
AUC	0.785 (0.689–0.880)	0.495 (0.378–0.613)	0.894 (0.822–0.965)
Cut-off (s)	6.55	2.48	2.42
Sensitivity (%) (95% CI)	76.5 (64.7–86.3)	27.5 (15.7–39.2)	86.3 (76.5–94.1)
Specificity (%) (95% CI)	75.6 (64.4–88.9)	84.4 (73.3–95.6)	88.9 (80.0–97.8)
PPV (%) (95% CI)	73.9 (58.9–85.7)	33.3 (14.6–57.0)	85.1 (71.7–93.8)
NPV (%) (95% CI)	78.0 (64.0–88.5)	49.3 (37.6–61.1)	89.8 (77.8–96.6)

AUC, area under the curve; PPV, positive predictive value; NPV, negative predictive value; CI, confid-ence interval; AT, arrival time; Diff, difference.

compared to the lesion AT, the TDOA excluded the influence of the patient's heart function (31), blood supply status of the lesion area, and injection rate of the contrast agent (26). In our study, the TDOA had a higher sensitivity and specificity than the lesion AT and the adjacent lung tissue AT. Based on TIC analysis, we generated many parameters such as TTP. No significant differences were found between the benign inflammation and malignant lesions group (**Table 2**). Our findings are distinct from previously reported data on the role of TTP (26). These results suggested that the diagnostic performance of TDOA was better than the conventional parameters. Furthermore, our results showed that there was no significant difference between the
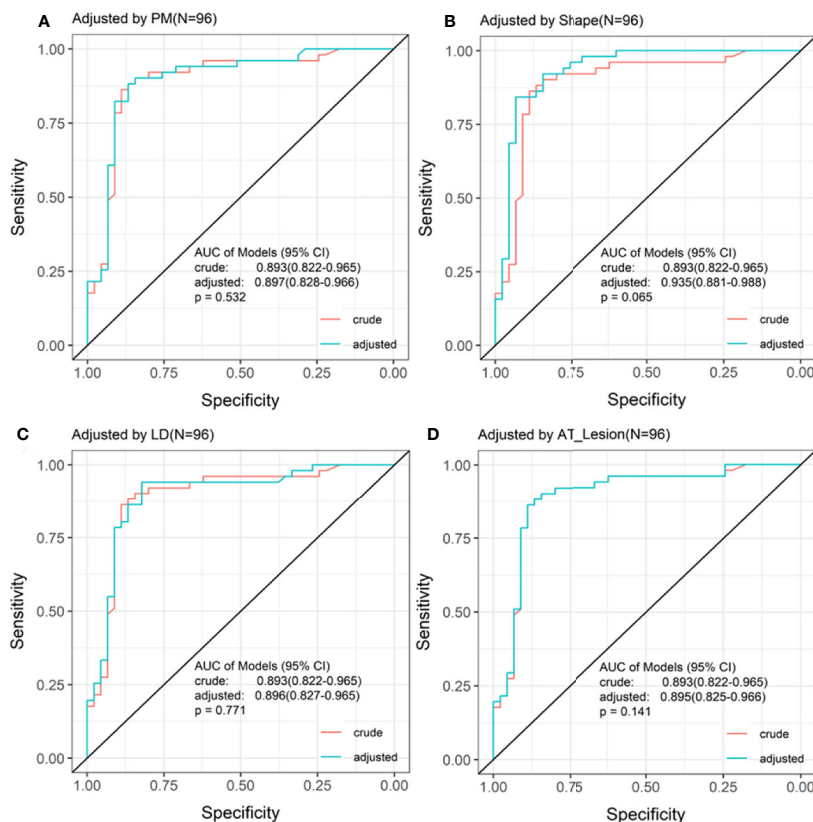
FIGURE 4 | Receiving operating characteristic (ROC) curve adjusted by the indices of patients. The ROC curve adjusted by the top four different indices for patients. There was no significant difference between crude ROC and adjusted ROC curve. AT, arrival time; PM, perfusion method.

crude and adjusted ROC curve, indicating that other indicators did not affect the diagnostic performance of TDOA.

Our study has some limitations. First, it was a single-center study and the number of patients was relatively small. Second, the major type of benign lesions were inflammation. More pathologic types of benign lesions are required to validate the applicability of TDOA. Last, it was a retrospective study.

CONCLUSIONS

We systemically analyzed and validated TDOA produced by CEUS to distinguish between benign inflammation and malignant PPLs with high diagnostic accuracy. These findings showed that the TDOA could be a feasible, sensitive, and specific method to diagnose PPLs.

DATA AVAILABILITY STATEMENT

The raw data supporting the conclusions of this article will be made available by the authors, without undue reservation.

ETHICS STATEMENT

The study was approved by the Ethics Committee of Dazhou Central Hospital (IRB00000003-19008). The Ethics Committee waived the need for patients to sign informed consent.

AUTHOR CONTRIBUTIONS

FXZ designed the study, revised the manuscript, and the figure. MT analyzed the CEUS parameters. QX drafted the manuscript and analyzed the data. JW analyzed the data. XYZ and JC revised the manuscript. HL collected the clinical characteristics and information. XXZ collected the clinical characteristics and information. GW analyzed the TICs. YT analyzed the TICs. FWZ organized the basic data. YC revised the manuscript and organized the basic data. JS recruited patients with PPLs and collected the clinical characteristics and information. All authors contributed to the article and approved the submitted version.

FUNDING

REFERENCES

1. Bray F, Ferlay J, Soerjomataram I, Siegel RL, Torre LA, Jemal A. Global cancer statistics 2018: GLOBOCAN estimates of incidence and mortality worldwide for 36 cancers in 185 countries. *CA Cancer J Clin* (2018) 68:394–424. doi: 10.3322/caac.21492

2. Akata S, Yoshimura M, Nishio R, Park J, Saito K, Uchida O, et al. High-resolution computed tomographic findings of small peripherally located squamous cell carcinoma. *Clin Imaging* (2008) 32:259–63. doi: 10.1016/j.clinimag.2007.10.002

3. Shah R, Sabanathan S, Richardson J, Mearns AJ, Goulden C. Results of surgical treatment of stage I and II lung cancer. *J Cardiovasc Surg (Torino)* (1996) 37:169–72.

4. Nesbitt JC, PJ Jr., Walsh GL, Roth JA, Mountain CF. Survival in early-stage non-small cell lung cancer. *Ann Thorac Surg* (1995) 60:466–72. doi: 10.1016/0003-4975(95)00169-L

5. Goldstraw P, Rami-Porta R, Asamura H, Ball D, Beer DG, Beyruti R, et al. The IASLC Lung Cancer Staging Project: Methodology and Validation Used in the Development of Proposals for Revision of the Stage Classification of NSCLC in the Forthcoming (Eighth) Edition of the TNM Classification of Lung Cancer. *J Thorac Oncol* (2016) 11:1433–46.

6. Mountain CF. Revisions in the International System for Staging Lung Cancer. *Chest* (1997) 111:1710–7. doi: 10.1378/chest.111.6.1710

7. Kono R, Fujimoto K, Terasaki H, Muller NL, Kato S, Sadohara J, et al. Dynamic MRI of solitary pulmonary nodules: comparison of enhancement patterns of malignant and benign small peripheral lung lesions. *AJR Am J Roentgenol* (2007) 188:26–36. doi: 10.2214/AJR.05.1446

8. Chu ZG, Sheng B, Liu MQ, Lv FJ, Li Q, Ouyang Y. Differential Diagnosis of Solitary Pulmonary Inflammatory Lesions and Peripheral Lung Cancers with Contrast-enhanced Computed Tomography. *Clinics (Sao Paulo)* (2016) 71:555–61. doi: 10.6061/clinics/2016(10)01

9. Dietrich CF, Kratzer W, Strobe D, Danse E, Fessl R, Bunk A, et al. Assessment of metastatic liver disease in patients with primary extrahepatic tumors by contrast-enhanced sonography versus CT and MRI. *World J Gastroenterol* (2006) 12:1699–705. doi: 10.3748/wjg.v12.i11.1699

10. National Lung Screening Trial Research T, Aberle DR, Adams AM, Berg CD, Black WC, Clapp JD, et al. Reduced lung-cancer mortality with low-dose computed tomographic screening. *N Engl J Med* (2011) 365:395–409. doi: 10.1056/NEJMoa1102873

11. Greenhill SR, Kovitz KL. *Flexible Bronchoscopy. 3rd ed.* The United States of America: Wiley-Blackwell (2012).

12. Salminen E, Niiniviita H, Järvinen H, Heinävaara SJAR. Cancer Death Risk Related to Radiation Exposure from Computed Tomography Scanning Among Testicular Cancer Patients. *Anticancer Res* (2017) 37:831–4. doi: 10.21873/anticanres.11385

13. Nordin AB, Sales S, Nielsen JW, Adler B, Bates DG, Kenney B. Standardized ultrasound templates for diagnosing appendicitis reduce annual imaging costs. *J Surg Res* (2018) 221:77–83. doi: 10.1016/j.jss.2017.07.002

14. Meier-Schroers M, Homsi R, Gieseke J, Schild HH, Thomas D. Lung cancer screening with MRI: Evaluation of MRI for lung cancer screening by comparison of LDCT- and MRI-derived Lung-RADS categories in the first two screening rounds. *Eur Radiol* (2019) 29:898–905. doi: 10.1007/s00330-018-5607-8

15. Pinsky PF, Bellinger CR, Miller DP. False-positive screens and lung cancer risk in the National Lung Screening Trial: Implications for shared decision-making. *J Med Screen* (2017) 25:110–2. doi: 10.1177/0969141317727771

16. Shen H. Low-dose CT for lung cancer screening: opportunities and challenges. *Front Med* (2017) 12:116–21. doi: 10.1007/s11684-017-0600-1

17. Baaklini WA, Reinoso MA, Gorin AB, Sharafkaneh A, Manian P. Diagnostic yield of fiberoptic bronchoscopy in evaluating solitary pulmonary nodules. *Chest* (2000) 117:1049–54. doi: 10.1378/chest.117.4.1049

18. Schreiber G, McCrory DC. Performance characteristics of different modalities for diagnosis of suspected lung cancer: summary of published evidence. *Chest* (2003) 123:115S–28S. doi: 10.1378/chest.123.1_suppl.115S

19. Dhillon SS, Harris K. Bronchoscopy for the diagnosis of peripheral lung lesions. *J Thorac Dis* (2017) 9:S1047–58. doi: 10.21037/jtd.2017.05.48

20. Schneider A, Johnson L, Goodwin M, Schelleman A, Bellomo R. Bench-to-bedside review: contrast enhanced ultrasonography–a promising technique to assess renal perfusion in the ICU. *Crit Care* (2011) 15:157. doi: 10.1186/cc10058

21. Correas JM, Bridal L, Lesavre A, Mejean A, Claudon M, Helenon O. Ultrasound contrast agents: properties, principles of action, tolerance, and artifacts. *Eur Radiol* (2001) 11:1316–28. doi: 10.1007/s003300100940

22. Steinl DC, Xu L, Khanicheh E, Ellertsdottir E, Ochoa-Espinosa A, Mitterhuber M, et al. Noninvasive Contrast-Enhanced Ultrasound Molecular Imaging Detects Myocardial Inflammatory Response in Autoimmune Myocarditis. *Circ Cardiovasc Imaging* (2016) 9:e004720. doi: 10.1161/CIRCIMAGING.116.004720

23. St Clair JR, Ramirez D, Passman S, Benninger RKP. Contrast-enhanced ultrasound measurement of pancreatic blood flow dynamics predicts type 1 diabetes progression in preclinical models. *Nat Commun* (2018) 9:1742. doi: 10.1038/s41467-018-03953-y

24. Nakamura J, Nakamura T, Deyama J, Fujioka D, Kawabata K, Obata JE, et al. Assessment of carotid plaque neovascularization using quantitative analysis of contrast-enhanced ultrasound imaging is useful for risk stratification in patients with coronary artery disease. *Int J Cardiol* (2015) 195:113–9. doi: 10.1016/j.ijcard.2015.05.107

25. Cao W, Cui S, Yang L, Wu C, Liu J, Yang F, et al. Contrast-Enhanced Ultrasound for Assessing Renal Perfusion Impairment and Predicting Acute Kidney Injury to Chronic Kidney Disease Progression. *Antioxid Redox Signal* (2017) 27:1397–411. doi: 10.1089/ars.2017.7006

26. Qureshi NR, Hintze C, Risse F, Kopp-Schneider A, Eberhardt R, Kauczor HU, et al. The feasibility of low mechanical index contrast enhanced ultrasound (CEUS) in distinguishing malignant from benign thoracic lesions. *Ultrasound Med Biol* (2011) 37:1747–54. doi: 10.1016/j.ultrasmedbio.2011.08.003

27. Hong-Xia Z, Wen H, Ling-Gang C, Wen-Jia C, Shuo L, Li-Juan D, et al. New Method for Discriminating between Bronchial and Pulmonary Arterial Phases using Contrast-Enhanced Ultrasound. *Ultrasound Med Biol* (2016) 42:1441–9. doi: 10.1016/j.ultrasmedbio.2016.01.029

28. Eldridge L, Moldobaeva A, Zhong Q, Jenkins J, Snyder M, Brown RH, et al. Bronchial Artery Angiogenesis Drives Lung Tumor Growth. *Cancer Res* (2016) 76:5962–9. doi: 10.1158/0008-5472.CAN-16-1131

29. Yin S, Cui Q, Wang S, Fan Z, Yan K. Analysis of Contrast-Enhanced Ultrasound Perfusion Patterns and Time-Intensity Curves for Metastatic Lymph Nodes From Lung Cancer: Preliminary Results. *J Ultrasound Med* (2018) 37:385–95. doi: 10.1002/jum.14345

30. Sperandeo M, Rea G, Grimaldi MA, Trovato F, Dimitri LM, Carnevale V. Contrast-enhanced ultrasound does not discriminate between community acquired pneumonia and lung cancer. *Thorax* (2017) 72:178–80. doi: 10.1136/thoraxjnl-2016-208913

31. Dietrich CF, Averkiou MA, Correas JM, Lassau N, Leen E, Piscaglia F. An EFSUMB introduction into Dynamic Contrast-Enhanced Ultrasound (DCE-US) for quantification of tumour perfusion. *Ultraschall Med* (2012) 33:344–51. doi: 10.1055/s-0032-1313026

SUPPLEMENTARY MATERIAL

The Supplementary Material for this article can be found online at: https://www.frontiersin.org/articles/10.3389/fonc.2020.578884/full#supplementary-material